

Spatial patterns and source attribution of urban methane in the Los Angeles Basin

Francesca M. Hopkins^{1*}, Eric A. Kort², Susan E. Bush³, James R. Ehleringer^{3,4}, Chun-Ta Lai⁵, Donald R. Blake⁶, James T. Randerson¹

¹Dept. of Earth System Science, University of California, Irvine, CA

²Dept. of Atmospheric, Ocean, and Space Sciences, University of Michigan, Ann Arbor, MI

³Dept. of Biology, University of Utah, Salt Lake City, UT

⁴Global Change and Sustainability Center, University of Utah, Salt Lake City, UT

⁵Dept. of Biology, San Diego State University, San Diego, CA

⁶Dept. of Chemistry, University of California, Irvine, CA

* Corresponding author: F.M. Hopkins, Dept. of Earth System Science, University of California, Irvine, Croul Hall 3100, Irvine, CA 92697, USA. (fhopkins@uci.edu)

- Atmospheric methane levels are highly variable across Los Angeles
- The majority of Los Angeles methane emissions are from fossil sources
- Mobile laboratory approach can identify and apportion methane emissions regionally

This is the author manuscript accepted for publication and has undergone full peer review but has not been through the copyediting, typesetting, pagination and proofreading process, which may lead to differences between this version and the Version of Record. Please cite this article as doi: [10.1002/2015JD024429](https://doi.org/10.1002/2015JD024429)

Abstract

Urban areas are increasingly recognized as a globally important source of methane to the atmosphere; however, the location of methane sources and relative contributions of source sectors are not well known. Recent atmospheric measurements in Los Angeles, California, USA, show that more than a third of the city's methane emissions are unaccounted for in inventories, and suggest fugitive fossil emissions are the unknown source. We made on-road measurements to quantify fine scale structure of methane and a suite of complementary trace gases across the Los Angeles Basin in June 2013. Enhanced methane levels were observed across the basin, but were unevenly distributed in space. We identified 213 methane hotspots from unknown emission sources. We made direct measurements of ethane to methane (C_2H_6/CH_4) ratios of known methane emission sources in the region, including cattle, geologic seeps, landfills, and compressed natural gas fueling stations, and used these ratios to determine the contribution of biogenic and fossil methane sources to unknown hotspots and to local urban background air. We found 75% of hotspots were of fossil origin, 20% were biogenic, and of 5% of indeterminate source. In regionally integrated air, we observed a wider range of C_2H_6/CH_4 values than observed previously. Fossil fuel sources accounted for 58-65% of methane emissions, with the range depending on the assumed C_2H_6/CH_4 ratio of source end-members and model structure. These surveys demonstrated the prevalence of fugitive methane emissions across the Los Angeles urban landscape, and suggested that un-inventoried methane sources were widely distributed and primarily of fossil origin.

1. Introduction

Methane (CH₄) is an important atmospheric pollutant: the second largest contributor to global warming, and a key constituent regulating CO and O₃ [Cicerone and Oremland, 1988]. Most sources of CH₄ to the atmosphere have been identified; however, their relative importance to the global budget is uncertain [Kirschke *et al.*, 2013]. CH₄ source budgets are even more uncertain at continental and regional scales [e.g., Kort *et al.*, 2008; Miller *et al.*, 2013]. The majority (50-65%) of CH₄ emissions globally come from anthropogenic sources, with a flux of approximately 330 Tg CH₄ per year [Kirschke *et al.*, 2013]. Reduction of CH₄ emissions has been suggested to be an effective short-term strategy to reduce global warming because of CH₄'s high radiative forcing relative to CO₂, around 28 times on a mass basis over a 100 y time horizon [Shindell *et al.*, 2012; Myhre *et al.*, 2013]. However, mitigation of anthropogenic CH₄ emissions requires an accurate CH₄ budget, including knowledge of location and sectoral contributions of different CH₄ emitters, particularly at scales where mitigation policies may be enacted [Hsu *et al.*, 2010; Jeong *et al.*, 2013].

Observations of elevated CH₄ levels in cities demonstrate that significant emissions of anthropogenic CH₄ are derived from urban areas [Blake *et al.*, 1984; Wunch *et al.*, 2009]. According to inventory estimates, 35% of the anthropogenic CH₄ in North America is emitted from urban regions [Marcotullio *et al.*, 2013]. However, recent atmospheric studies at the state

and city levels in California suggest a 30-80% underestimation of CH₄ emissions in the state greenhouse gas inventory, using stationary and airborne trace gas measurements [Wunch *et al.*, 2009; Hsu *et al.*, 2010; Wennberg *et al.*, 2012; Jeong *et al.*, 2013; Peischl *et al.*, 2013; Wong *et al.*, 2015]. Uncounted fugitive emissions, such as leaks from natural gas pipelines, are hypothesized to account for this mismatch between bottom-up inventories and top-down measurements [Brandt *et al.*, 2014]. On road surveys in major cities such as Boston and Washington, DC have revealed large fugitive leaks from natural gas distribution pipelines [Phillips *et al.*, 2013; Jackson *et al.*, 2014]. In addition to extensive natural gas pipeline networks, cities have a variety of other CH₄ sources, including landfills, water treatment plants, natural gas vehicles and infrastructure, and in the case of Los Angeles, fossil fuel extraction and refining, and dairy agriculture. Fugitive emissions may also originate from these sectors. The heterogeneous mixture of source sectors in the urban environment complicates stationary and aircraft measurements of trace gases that cannot resolve fine-scale structure at the source level. Extensive road networks in cities enable vehicle coverage over large areas, providing a method for measuring the spatial distribution of CH₄ emissions. On road sampling of surface trace gas enhancement can locate CH₄ emission hotspots and attribute CH₄ enhancements to source sectors, and aid in interpretation of stationary or remotely sensed measurements [e.g., Petron *et al.*, 2012; Leifer *et al.*, 2013].

In the U.S., the two largest sources of urban CH₄ emissions are waste disposal and natural gas systems [US EPA, 2014]. These two sources represent the two primary pathways by which CH₄ is produced—biogenic and thermogenic. Waste disposal, in landfills and wastewater

treatment plants, produces biogenic CH₄ as a result of microbial decomposition of organic matter under anaerobic conditions. Biogenic CH₄ is also produced in the gut of livestock, and from manure. In contrast, thermogenic CH₄ originates from the geologic processes that create all fossil fuels, and is present in fossil fuel deposits including coal beds, oil fields, and geologic seeps [Etioppe and Ciccioli, 2009]. Thermogenic CH₄ also is emitted through intentional venting and fugitive leaks in the extraction, storage, refining, transport and use of natural gas. Incomplete combustion of fuels represents a third pathway for CH₄ production; pyrogenic sources are also a minor component (<2%) of CH₄ emissions [US EPA, 2014]. Both thermogenic and pyrogenic sources of CH₄ also emit more complex hydrocarbons, including ethane (C₂H₆), whereas biogenic sources do not [Rudolph, 1995; Kirchstetter et al., 1996; Etioppe and Ciccioli, 2009]. Hence, elevated CH₄ accompanied by elevated C₂H₆ values can be used as a tracer of fossil fuel sources of CH₄ [e.g., Aydin et al., 2011].

In the Los Angeles Basin, evidence from stable isotopes of CH₄ and measurements of higher hydrocarbons (e.g., C₂H₆, propane, butane) suggest that fossil emissions are the predominant source of CH₄ [Townsend-Small et al., 2012; Wennberg et al., 2012; Peischl et al., 2013]. Specifically, leakage from natural gas infrastructure [Wennberg et al., 2012] and from local fossil CH₄ sources [Peischl et al., 2013] are thought to be the most important contributors. However, the complex geologic setting and intense human impact within the basin complicate CH₄ source attribution in the Los Angeles area. The Los Angeles region is known for naturally occurring geologic seeps, such as the La Brea Tar Pits, as well as extensive oil drilling taking place during the last century and continuing to the present day [Bilodeau et al., 2007]. In

addition, Los Angeles is a major industrial and shipping center, with more than 10 oil refineries and storage facilities. The number of producing wells in the basin has decreased since the 1960s; however the number has increased anew over the past decade with application of enhanced oil recovery techniques such as hydraulic fracturing [Cardno *ENTRIX*, 2012; Gautier *et al.*, 2012; Tennyson, 2005]. Industrial centers, such as the Port of Los Angeles, the Harbor area, the surroundings of Los Angeles International Airport (LAX), and downtown were constructed near or over major oil fields (Figure 1a) meaning that many anthropogenic sources of CH₄ are co-located with each other and with potential geologic CH₄ sources.

Missing from stationary or airborne measurements is detailed spatial information about the distribution of CH₄ sources that is needed for developing monitoring and mitigation strategies for urban CH₄ emissions. Here we present data from an extensive on-road survey of CH₄ levels in the Los Angeles Basin during June 2013. Our goals were twofold: to describe the spatial patterns of CH₄ and other trace gases with urban sources in the Los Angeles Basin, and to use local measurements of the C₂H₆ to CH₄ ratio to attribute sources of fugitive CH₄ emissions, measured as hotspots and in local background air. We demonstrate the utility of mobile surveys to locate and attribute urban CH₄ hotspots, and of complementary measurements of C₂H₆ to perform a regional source apportionment.

2. Methods

2.1 Instrumentation

We used a mobile observatory system to continuously survey trace gas mole fractions on-road while also recording global position and winds. The platform was a 2011 Ford Transit Connect van with a modified electrical system and sampling mast that extended to 3.5 m above the road surface located just behind the driver's seat of the vehicle [Bush *et al.*, 2015].

The observatory was equipped with two cavity ring-down spectrometers (Picarro Inc., Sunnyvale, California), one measuring CH₄, CO₂, and H₂O (G1301), and the other measuring CO, CO₂, and H₂O (G1302). The instruments were plumbed in serial, sampling air from a common inlet located at the top of the sampling mast. Outside air was pumped continuously through the line at a rate of 4.2 L per minute. The G1301 measured every 2-3 seconds, and the G1302, every 3-4 seconds. The time delay for measurement of outside air ranged from 0.7-3 seconds, depending on the variable instrument sampling rate. During this campaign, the laboratory also had an Aerodyne Ethane Mini Monitor quantum cascade laser spectrometer on board to measure C₂H₆ and CH₄ [Yacovitch *et al.*, 2014]. The Ethane Mini Monitor sampled from a separate inlet line to enable instrument background scans by purging with N₂ for 30 seconds every 15 minutes. In addition, the instrument measured a reference C₂H₆ cell for 3 seconds every 2 minutes to maintain a line-lock on the C₂H₆ spectral feature. Apart from reference and background scan times, data were collected once a second, with a 1 second response time.

Position data were collected every 5 seconds by a GPS16X-HVS receiver (Garmin International, Inc., Olathe, Kansas) mounted on the vehicle's roof, and wind direction and speed

were measured with a Weather Station WS-200WM (Airmar Technology Corp., Milford, New Hampshire) mounted to the top of the sampling mast.

2.2 Calibration

We calibrated measurements made by cavity ring-down trace gas spectrometer using two NOAA-certified air standards that contained known amounts of CO₂, CO, and CH₄. Standards were measured for several minutes before and after each transect, with each transect defined as a set of on-road measurements made over the course of several hours. The relationship between known and measured standard values was applied as a linear correction to the data collected during that transect. Measurement precision was 1.7 ppm for CO₂, 2.1 ppb for CH₄, and 8 ppb for CO based on the standard deviation of all measured standards for the campaign. For CH₄, G1301 performance was found to be linear over a range of standard values from 1.7 to 10 ppm. Reported CH₄ values greater than 10 ppm hence represent an approximation (<0.01% of data reported here).

We report C₂H₆ data as spectroscopic mole fraction, which has an expected 1 second precision of 0.1 ppb in on a moving mobile laboratory platform [Yacovitch *et al.*, 2014]. We checked the accuracy of spectroscopic C₂H₆ by comparing it to C₂H₆ measured in the laboratory on 5 simultaneous whole air samples that were taken during periods when atmospheric C₂H₆ was relatively constant. The average of spectroscopic C₂H₆ from the whole air sampling period was within 10% of reported C₂H₆ values by gas chromatography-flame ionization detector [Colman *et al.*, 2001].

2.3 Data processing

Original data were collected at varying frequencies for each instrument ranging from once every second (Aerodyne Mini Monitor) to once every 3-4 seconds (Picarro G1302). We used correlation analysis of the two CO₂ data streams to adjust for time delays between the two Picarro instruments, and CH₄ correlations to adjust for time delays between the Aerodyne Mini Monitor and Picarro G1301. All data were subsequently averaged to 5-second intervals.

For spatial analyses, 5-second averaged data were spatially gridded along 150 m road intervals by averaging observations taken within this increment. 150 m segments were chosen to maximize the information content of gridded data; less than 3% of the 150 m segments required linear interpolation of the nearest neighbors to fill in gaps in data.

2.4 Background trace gas mole fractions

We determined urban excess values for each trace gas species by subtracting an estimated clean air background mole fraction from trace gas-enriched measurements made in polluted urban air, following *Blake et al.* [1984]. We estimated the clean air background value for each trace gas by selecting the minimum observation for each transect in the study period, and then averaging the lowest 20% of these transect minimums (i.e., the lowest 4 out of 21 transects). We estimated the uncertainty in background values as the standard deviation of the minimum trace gas measurement from all transects within the basin (n=21). The background value for CH₄ was 1821 ± 24 ppb, CO was 80 ± 24 ppb, CO₂ was 396.3 ± 3.2 ppm, and C₂H₆ was 0.6 ± 0.2 ppb. Background values measured in the basin were all within 1 standard deviation of values reported at Kumukahi, Hawaii in June 2013 (June 2009 for C₂H₆) by NOAA's Global

Greenhouse Reference Network [Helmig *et al.*, 2011; Dlugokencky *et al.*, 2013a, 2013b; Novelli and Masarie, 2013]. At Kumukahi, CH₄ was 1836 ± 7 ppb, CO was 85 ± 5 ppb, CO₂ was 399.8 ± 0.7 ppm, from the average of flask samples on 8 measurement days in June 2013, and C₂H₆ was 0.6 ± 0.1 ppb from the average of flask samples from 5 measurement days in June 2009. The background value for C₂H₆ was similar to observations made from aircraft above the Los Angeles Basin, 0.6 ± 0.3 ppb for the lowest values on three measurement days that coincided with on-road sampling.

2.5 Observations

We sampled approximately 1900 km of road in the Los Angeles Basin, in June and early July of 2013 (Figure 1). We conducted 21 transects, with each transect defined as a set of on-road measurements made within a specific time period (e.g., midday on June 15). Most routes were repeated a minimum of two times, at midday (10 am to 4 pm) and after nightfall (9 pm to 1 am).

Transect routes were designed to characterize the C₂H₆/CH₄ ratios of known biogenic and fossil CH₄ sources, including landfills, wastewater treatment facilities, and livestock, and oil fields and refineries, natural gas storage and distribution infrastructure, and geologic sources, respectively (Figure 1a: map image of known CH₄ emitters in Los Angeles Basin). We also designed transect routes to cover common land use types within the Los Angeles Basin, with varying degrees of human influence (urbanization).

On June 17-19, we coordinated on-road sampling to cover the same locations at approximately the same time as a concurrent aircraft campaign. The aircraft was a DC-8 flown out of NASA's Dryden Flight Research Center over the Los Angeles Basin as part of the NASA

Student Airborne Research Program (www.nserc.und.edu/sarp/sarp-2009-2013/2013). During flight, whole air samples were taken in evacuated 2L stainless steel canisters. Canister samples were analyzed in the laboratory for CH₄, C₂H₆, CO, and CO₂ mole fractions and along with other constituents by gas chromatography-flame ionization detector [Colman *et al.*, 2001]. We included only samples taken over land in the Los Angeles Basin at less than 3000 feet (914 m) above ground level in this analysis.

2.6 Hotspot identification

Plumes of air containing CH₄ values that exceeded the 95th percentile of CH₄ observations for that transect were considered indicators of a CH₄ hotspot. Some hotspots coincided with known emissions sources (shown in Figure 1a), while others were of an unknown origin. We defined hotspots as road segments where at least one 150 m segment had a CH₄ value that exceeded the 95th percentile threshold (132 to 360 ppb above the local background level). The spatial extent of each hotspot was defined by the number of adjacent 150 m road segments that had CH₄ values above the local background level. Local background CH₄ levels varied over the course of each transect due to spatial variability and diurnal changes in boundary layer height, and were thus determined by visual inspection of each transect. We approximated the amount of local CH₄ enhancement by summing excess CH₄ above the local background level (i.e., area under the curve) for each hotspot.

2.7 Source apportionment

We used the range of mole fraction ratios of excess C₂H₆ to excess CH₄ from known CH₄ emission sources to apportion CH₄ in hotspots of unknown origin, and for local background air

measured away from CH₄ hotspots, representing a regional mix of CH₄ source sectors. We used linear regression on excess C₂H₆ and excess CH₄ observations from CH₄ hotspots of known emitters to determine the range of C₂H₆/CH₄ ratios that characterized biogenic and fossil sources. Regression slope estimates included uncertainty in background mole fractions, estimated as 1 standard deviation of background levels [York *et al.*, 2004]. In theory, biogenic sources should have a ratio of 0 (i.e., no concurrent C₂H₆ production). In practice, many primarily biogenic sources had small but significant positive ratios because of measurement uncertainties and a small amount of contribution from nearby or co-located fossil sources. We used the observed range of excess C₂H₆ to excess CH₄, hereafter denoted C₂H₆/CH₄, from known sources to determine the likely origins of unknown hotspots based on their C₂H₆/CH₄ slopes. For regional source apportionment, we included only observations of local background air measured away from CH₄ hotspots, where we assume the air is well-mixed with respect to CH₄, and hence representative of a mix of urban CH₄ sources across the Los Angeles Basin.

3. Results

3.1 Spatial distribution of CH₄ and C₂H₆ across the Los Angeles Basin

CH₄ mole fractions were highly variable across the Los Angeles Basin, ranging from near background levels to 58 ppm measured at the Clean Trucks compressed natural gas (CNG) fueling station in the Port of Long Beach (Figure 1b, Map S1). We observed local CH₄ enrichment (hotspots) in the vicinity of many known CH₄ emission sources, including active and closed landfills, cattle operations, water treatment facilities, geologic seeps, oil extraction and

refining facilities, natural gas infrastructure, and gas-fired power plants (Tables 1-3). We also observed many CH₄ hotspots of an unknown origin, including local enrichment of about 5 times background levels in a discrete, high CH₄ event. Elevated levels of atmospheric C₂H₆ were also observed in many, but not all locations where CH₄ enhancements were observed (Figure 1c).

Local CH₄ background levels, excluding known and unknown CH₄ hotspots, varied across the region (Figure 1b). In general, local CH₄ background levels were higher in inland parts of the basin. For example, local background CH₄ levels in Riverside were twice as high as they were in Irvine for the same day, three times as high in Ontario, and four times as high in Pasadena. Inland areas tend to accumulate polluted air generated in the basin due to prevalent onshore winds during spring and summer [e.g., *Vutukuru et al.*, 2006; *Peischl et al.*, 2013]. Local CH₄ levels tended also to be higher in more urbanized areas of the basin, such as near downtown Los Angeles.

C₂H₆ also increased along a coast-to-inland gradient in a manner similar to CH₄, with large areas of enrichment located in downtown Los Angeles, around the Long Beach oil field, and in the city of Ontario (Figure 1c). C₂H₆ mole fractions ranged from background levels similar to those observed in remote ocean regions to 2370 ppb measured at the La Brea Tar Pits. Local background levels of C₂H₆ varied even more than for CH₄, with levels four-fold higher in Riverside and six-fold higher in Pasadena than in Irvine, and up to 20 times higher in Ontario. The greater urban enhancements of C₂H₆ compared to CH₄ were likely driven by significant urban C₂H₆ emissions and lower remote background mole fractions as a consequence of a shorter lifetime (approximately 2 months for C₂H₆ vs. >10 y for CH₄), and little C₂H₆ production in

remote ocean regions [Xiao *et al.*, 2008]. The ratio of C_2H_6 to CH_4 was also highly variable across the region. In particular, C_2H_6/CH_4 was markedly higher along surface streets in dense, highly urbanized areas near downtown Los Angeles and central Orange County (Figure 1d, Map S1).

3.2 C_2H_6/CH_4 ratio of known emitters

We made measurements of CH_4 and C_2H_6 at known CH_4 emissions sources to characterize the C_2H_6/CH_4 ratios of biogenic and fossil end-members, and to enable subsequent use of this information to apportion CH_4 emission sources in the Los Angeles Basin. We calculated C_2H_6/CH_4 ratios for each known CH_4 emitter, and subsequently for each source sector as the slope of a line fit through a plot of excess C_2H_6 vs. excess CH_4 using a minimization of orthogonal distance and including measurement error in both variables (Table 1-3). The C_2H_6/CH_4 ratio for biogenic sources ranged from -0.05 ± 0.08 % for former landfills to 0.02 ± 0.01 % for water treatment facilities (Table 4). Most biogenic CH_4 emitters did not have statistically significant C_2H_6/CH_4 slopes (i.e., slopes were not statistically different from 0), except for the Puente Hills landfill and several water treatment facilities (Table 1). Significant C_2H_6/CH_4 slope values were likely caused by collocated fossil emissions. For example, fossil-derived natural gas and biogenic CH_4 may be combined to fuel natural gas vehicles. Both the Puente Hills landfill and the Orange County Sanitation District water treatment plant had CNG fueling stations on site.

Known fossil sources of CH_4 were grouped into two categories based on their expected C_2H_6/CH_4 ratios: (1) fugitive leaks of pipeline-quality natural gas, which include emissions from

gas-fired power plants, CNG fueling stations, and natural gas pipelines (Table 2), and (2) unprocessed geologic CH₄ sources, including oil fields, oil refineries, and geologic seeps (Table 3). Previous studies have shown a relatively narrow range of C₂H₆/CH₄ ratios for pipeline natural gas compared to geologic CH₄ sources [Jeffrey *et al.*, 1991; Wennberg *et al.*, 2012]. Fugitive natural gas leaks for sources sampled in this campaign had C₂H₆/CH₄ ratios ranging from 1.5 ± 0.3 % for CNG fueling stations to 3.1 ± 0.9 % for natural gas-fired power plants (Table 4). Among pipeline gas sources, all C₂H₆/CH₄ slopes were statistically significant at the p<0.05 level except for one power plant sample with few (n=5) measurements (Table 2). This range is consistent with direct measurements of C₂H₆/CH₄ in pipeline gas in Southern California, 1.33-2.59%, reported by Wennberg *et al.* [2012]. C₂H₆/CH₄ ratios for geologic CH₄ sources tended to be higher than for pipeline gas, ranging from 1.4 ± 0.1 % for geologic seeps to 3.4 ± 5.0 % for oil fields (Table 4). However, the range of C₂H₆/CH₄ ratios for individual geologic sources was very broad, spanning -0.1 ± 0.1 % to 9 ± 5 % for oil fields, and 0.01 ± 0.02 % to 4.0 ± 0.1 % for geologic seeps (Table 3). These C₂H₆/CH₄ values were consistent with previous observations in oil fields, 0.7-12.0%, and geologic seeps, 0.8-7.5%, in the Los Angeles Basin [Jeffrey *et al.*, 1991]. Several geologic sources had C₂H₆/CH₄ ratios similar to biogenic sources (e.g., Newport Beach oil field, geologic seeps in Newport Beach and Playa Vista), and may be due to biodegradation of higher hydrocarbons or mixing of thermogenic and biogenic natural gas, both of which have been observed in the Los Angeles Basin [Jeffrey *et al.*, 1991].

3.3 Distribution of CH₄ and other trace gases

Atmospheric levels of trace gases were distributed unevenly across the basin, with high CH₄ (and C₂H₆) values concentrated in CH₄ hotspots (Figure 1). We compared the spatial distributions of the four measured gases with urban sources by their Gini coefficients, where 0 represents a perfectly equal distribution, and 1 represents a perfectly unequal distribution [Gini, 1912]. CH₄ was the most unevenly distributed trace gas over the basin, with a Gini coefficient of 0.55, followed by C₂H₆, 0.47; CO, 0.42; and CO₂, 0.39.

To better understand patterns of emission variability, particularly for CH₄ hotspots of unknown origin, we removed data collected in CH₄ hotspots associated with known emission sources from further analysis. This subset of data comprised about 5.9% of total distance covered in the campaign. We then sorted and ranked the remaining 94.1% of the observations according to their contribution to the total excess measured during the campaign (Figure 2). A considerable amount of excess CH₄ measured in the Los Angeles Basin was associated with CH₄ hotspots from unknown sources. Just 1% of total distance traveled, excluding CH₄ hotspots of known emission sources, accounted for 8% of excess CH₄ measured across the basin. Similarly, the top 5% of distance traveled by CH₄ mole fraction was responsible for 21% of total excess CH₄. Hotspots also contributed disproportionately to trace gas excess for C₂H₆ and CO; the top 1% of transect increments accounted for 7% of total excess C₂H₆, and 8% of total excess CO. CO₂ was the most evenly distributed trace gas, with the top 1% of transect distance with respect to CO₂ accounting for just 4% of total excess CO₂.

3.4 Variability in spatial patterns over time

We used repeated measurements of a section of the Pacific Coast Highway between Newport Beach and Seal Beach to determine how spatial patterns in atmospheric trace gas levels varied with time, and under different wind conditions. We observed many CH₄ hotspots in the same location across 4 different sampling days at 4 different times of day, despite differences in wind speed and direction (Figure 3).

We calculated the correlation coefficient for trace gas mole fractions between the 4 complete transects to quantify the repeatability of trace gas observations. CH₄ was highly correlated in space among all 4 transects runs (correlation p values <0.004), with an average correlation coefficient of 0.24, and a maximum correlation of 0.51 between the afternoon and night transects. These correlations were highly significant, given the large number of 150 m road segments on each transect (n=174). CO₂ was also well correlated among transects, with an average of 0.21, and a maximum correlation coefficient of 0.47 between the noon and evening transects. CO had the lowest average correlation across transects pairs, with significant correlation observed for only 3 of 6 transect combinations (p<0.05). The high spatial correlation of CH₄ values on repeated transects was consistent with emissions from persistent point sources, whereas lower correlations for CO₂ and CO were consistent with more variable traffic emissions.

Trace gas excess mole fractions varied over the course of the day, with a different pattern observed for CH₄ than for CO and CO₂. CH₄ mole fractions were lowest during midday, and highest at night. This pattern was consistent with a higher planetary boundary layer and a well-mixed atmosphere in the afternoon that reduced local CH₄ levels, and more stable atmospheric conditions at night that trapped CH₄ emissions near the surface. Diurnal patterns of CO and CO₂

were subject to the same boundary layer effect; however, the highest values of CO and CO₂ along this transect were observed in the 5-6 pm period, suggesting a time-varying emissions source that was consistent with increased vehicle emissions during the evening rush hour.

The lowest trace gas excess values in this section of the Pacific Coast Highway were consistently measured while passing the Bolsa Chica Ecological Reserve, a salt marsh nature preserve (located between km 6 and km 12 of this road section and marked in orange on the map panel of Figure 3). Reductions in trace gas levels around the marsh were particularly pronounced for CH₄. No CH₄ hotspots were observed in this area, suggesting that CH₄ hotspots originated from built-up urban areas. Despite differences in wind direction and speed among measurement time periods, the consistently low CH₄ mole fractions measured in the vicinity of Bolsa Chica demonstrate the sensitivity of the measurement technique to local emissions, and provided qualitative evidence that the measurement footprint of observed hotspots in other parts of the basin was on the order of several km or less.

3.5 Trace gas ratios of unknown hotspots and local background air

Both C₂H₆ and CH₄ were unevenly distributed in space; however, some of the locations with the highest CH₄ values were unmatched by C₂H₆ (Figure 4). The top 3% of transect distance with respect to CH₄ values contained 15% of excess CH₄ including unknown hotspots and local background air, but only 10% of excess C₂H₆, suggesting a spatially varying combination of sources across the basin. To visualize this mixture, we calculated the ratio between C₂H₆ and CH₄, and between CO and CO₂ for every 150 m transect segment, and plotted the ratios as a fraction of total CH₄ or CO₂ excess (Figure 5). The bimodal C₂H₆/CH₄ distribution suggests two

different source processes contributing to atmospheric CH₄ observations, with a small peak centered on a C₂H₆/CH₄ mole ratio less than 0.5%, reflecting biogenic CH₄ sources, and a second, broad peak, centered on 1.2%, reflecting fossil CH₄ sources (Figure 5a). Much of the distribution falls along the expected ratio for natural gas in the Los Angeles Basin, 1.33-2.59%, reported by Wennberg *et al.*, [2012].

In contrast, a plot of the ratio of CO to CO₂ had only one peak, centered between 0.44% and 0.66% (Figure 5b). This distribution is similar to CO/CO₂ ratios measured in Irvine during the winter of 2007-2008 by Djuricin *et al.* [2010] (0.65-1.0%), and the range observed in Pasadena during summer of 2010 by Newman *et al.* [2013] (0.2-2.0%). Very little excess CO₂ (1%) had a CO/CO₂ ratio less than 0.2%, as would be expected from biogenic CO₂ sources. Hence the CO/CO₂ ratio suggests that the vast majority of CO₂ measured during the on-road campaign is not representative of terrestrial ecosystem sources, and observed variation was likely driven by combustion sources.

3.6 Source apportionment of unknown hotspots

We used C₂H₆/CH₄ ratios to apportion excess CH₄ measured at hotspots of unknown origin to biogenic and fossil sources (Figure 6). Unknown CH₄ hotspots, defined as spatially contiguous observations where at least one CH₄ observation exceeded the 95th percentile for that transect with no obvious emission source, comprised 5.8% of total distance traveled. We used the highest C₂H₆/CH₄ ratio observed for known biogenic sources, 0.50%, as the upper limit for possible C₂H₆/CH₄ ratios from unknown biogenic sources. C₂H₆/CH₄ slopes for CH₄ hotspots falling beneath this value were classified as biogenic. Similarly, we used the lowest C₂H₆/CH₄

excess ratio measured from fugitive natural gas sources, 0.87%, as the lower limit for identifying fossil-derived CH₄ sources. 40 of 213 unknown hotspots were biogenic, 161 were fossil, and 11 had an intermediate slope, and hence were considered indistinguishable.

3.7 Source apportionment of urban background air

The remaining 88.3% of distance traveled, excluding known and unknown CH₄ hotspots, was assumed to represent a more integrated measurement of excess CH₄ sources across the basin. The C₂H₆/CH₄ ratio measured in these samples was similar to that measured by aircraft over the same locations during three days of coincident sampling (Figure 7); 3.1 ± 0.8 % for aircraft vs. 3.2 ± 0.1 % for on-road on June 17, 1.6 ± 0.3 % for aircraft vs. 1.4 ± 0.2 % for on-road on June 18, and 1.7 ± 1.2 % for aircraft vs. 2.7 ± 0.6 % for on-road on June 19. C₂H₆/CH₄ values of this well-mixed, local background air were often higher than the minimum C₂H₆/CH₄ ratio observed for natural gas sources, suggesting that most of excess CH₄ present in urban air was fossil derived (Figure 7).

To apportion CH₄ sources in local background air, we compared observed C₂H₆/CH₄ ratios to simulated C₂H₆/CH₄ values for varying proportions of biogenic and fossil CH₄ inputs. We represented C₂H₆/CH₄ values of biogenic sources as a random, normal distribution with a mean of 0%, and a standard deviation of 0.03%, based on the average and standard error of C₂H₆/CH₄ values observed at known biogenic hotspots. Similarly, we constructed a normal distribution of C₂H₆/CH₄ values with a mean of 2.5% and standard deviation of 1.1% for fossil sources (Table 4). We determined the fossil fraction that best simulated the observed local background C₂H₆/CH₄ distribution by performing 15000 mixing trials for each fossil fraction,

ranging from 0-1, with end-member ratios randomly selected using the mean and standard deviations of biogenic and fossil emission ratio data described above. We found that a mean fossil fraction of 62% (59-64%) best matched C_2H_6/CH_4 values in local background air according to Kolmogorov-Smirnov and Cramer-von Mises test statistics. The range of simulated fossil fraction values includes uncertainty in measured and background CH_4 and C_2H_6 values, by refitting simulations to C_2H_6/CH_4 observations plus or minus propagated error from those sources.

In addition to measurement error, variation in C_2H_6/CH_4 end-member values introduces uncertainty into the inferred fossil fraction. We examined the role of this variation by performing similar simulations to those described above, but assuming different fossil end-member C_2H_6/CH_4 values (we do not expect biogenic end-members to differ from 0). Modifying the fossil fraction to reflect only natural gas sources (mean and standard deviation of 2.2 ± 0.4 %), the optimal fossil fraction increased to 64%. For the case of only geologic sources (mean and standard deviation of 2.8 ± 1.4 %), the inferred fossil fraction decreased to 58%. Nevertheless, neither of these scenarios was able to match the data as well as the fossil end-member that includes both sources (Figure 8). We also separately simulated three hypothesized CH_4 sources: biogenic, natural gas, and geologic, with the same C_2H_6/CH_4 values used in the two-source simulations. The combination of three sources had a best fit fossil fraction of 65% (Figure 8), and was better able to reproduce the high frequency of C_2H_6/CH_4 values clustered around 1.2%, as well as the large variability in C_2H_6/CH_4 greater than 3%. However, the three-source mixture case is poorly constrained because of the need to fit additional parameters.

4. Discussion

4.1 Methane source apportionment in Los Angeles

Mobile laboratory on-road sampling enabled us to make high frequency, local-scale measurements of multiple trace gases across the Los Angeles Megacity region. We directly measured emission ratios of different sources, at the scale of individual facilities, and simultaneously obtained regionally integrated measurements of multiple trace gases in the urban air mass. Highly spatially resolved CH_4 and C_2H_6 data allowed us to determine the relative contributions of different emissions sectors to regional urban CH_4 excess. These data offer further evidence for an under-inventoried and dispersed set of fossil CH_4 sources to the Los Angeles atmosphere. We also identified targets for future work and potential mitigation of CH_4 emissions.

We measured CH_4 enrichment at 33 individual point sources to determine the range of $\text{C}_2\text{H}_6/\text{CH}_4$ ratios for biogenic or fossil sources. As expected, observed $\text{C}_2\text{H}_6/\text{CH}_4$ of known biogenic sources tended to be very low compared to other observations, despite a few locations with higher than expected C_2H_6 levels (e.g., Orange County Sanitation District Water Reclamation Plant). Known fossil CH_4 emissions sources had varied $\text{C}_2\text{H}_6/\text{CH}_4$ signatures, reflecting the wide range of $\text{C}_2\text{H}_6/\text{CH}_4$ signatures of geologic sources in the basin. In contrast, local background air had a $\text{C}_2\text{H}_6/\text{CH}_4$ signature distinct from hotspot biogenic and fossil sources, clearly showing contributions of natural gas and oil sources of CH_4 .

Our attribution of 62% of Los Angeles CH₄ to fossil sources, with a possible range of 58-65%, is within the range of other studies using atmospheric C₂H₆/CH₄ measurements in Los Angeles, with estimates of 56% by *Peischl et al.* [2013], and 70% by *Wennberg et al.* [2012]. Our analysis gives insight into why such a large range has been inferred by previous work. First, we found that the inferred contribution of fossil sources depends strongly on the choice of the C₂H₆/CH₄ ratio of the fossil end-member. *Wennberg et al.* [2012] hypothesized that the majority of CH₄ in the Los Angeles Basin originated from leaks of pipeline natural gas, and may have overestimated the fossil contribution by assuming all fossil CH₄ had a C₂H₆/CH₄ ratio representative of natural gas. In contrast to aircraft measurements, our sample of urban air had a much wider range of C₂H₆/CH₄ values that are outside the range of natural gas sources measured here or in previous work in the region [*Wennberg et al.*, 2012], demonstrating that fossil CH₄ sources in the Los Angeles Basin must be a mixture of pipeline and unprocessed gas emissions.

Most of the variability in fossil C₂H₆/CH₄ ratios we observed is likely to stem from the large variation in geologic CH₄ sources, which ranged from 0 to 9%. We found that geologic seeps had particularly low C₂H₆/CH₄ values, with two out of three surveyed geologic seeps with C₂H₆/CH₄ values <0.15%. Hence geologic sources may be confounded for biogenic sources without specific knowledge of the emission source in a particular location. It is possible that the analysis of *Peischl et al.* [2013] underestimated geologic emissions, as some geologic seeps have C₂H₆/CH₄ ratios that are indistinguishable from biogenic sources.

4.2 Strengths and weaknesses of mobile laboratory technique

Discrepancies between top-down measurements and bottom-up inventories present a major challenge for greenhouse gas mitigation policy and planning, particularly for CH₄. Mobile laboratories are particularly suited for addressing this challenge, having the ability to make complementary regional top-down CH₄ measurements [Petron *et al.*, 2012] and facility-level bottom-up measurements [Jackson *et al.*, 2014]. In this study, regional C₂H₆/CH₄ apportionment of local background air demonstrated that the predominant source of CH₄ emissions is fossil. We also found that the majority of unknown CH₄ hotspots were of fossil origin, providing further evidence for the importance of dispersed, fugitive fossil CH₄ emissions in the Los Angeles Basin. These CH₄ hotspots of unknown source represent an important target for future research. Repeated measurements of these unknown hotspots are needed to determine whether they persist in time, and with tools that can pinpoint the precise locations of CH₄ leaks for source attribution.

Our regional apportionment attributed a large portion of CH₄ in the Los Angeles atmosphere to emissions of pipeline-quality natural gas; however, we observed few discrete leaks from natural gas pipelines. This contrasts with recent observations of frequent pipeline leaks detected by on road sampling in Boston and Washington, DC [Phillips *et al.*, 2013; Jackson *et al.*, 2014], and is consistent with recent work showing relatively fewer pipeline gas leaks in the western U.S. [Lamb *et al.*, 2015]. Fugitive gas emissions in those cities were found in areas with cast-iron gas mains, which are not present in Los Angeles [Southern California Gas Company, 2011]. The most significant fugitive emissions of natural gas we observed came from compressed natural gas fueling stations. Fugitive emissions associated with natural gas fueling infrastructure are not currently included in the California Air Resources Board inventory or in prominent life cycle

assessment models [CARB, 2014; A. Burnham, personal communication]. A better understanding of which components of CNG fueling are leaking is needed for emissions quantification and mitigation.

Closed landfill sites also had surprisingly large emissions, with measureable increases in atmospheric CH₄ levels near most sites surveyed (Table 1). Atmospheric CH₄ enhancements were also observed at active and several closed landfill sites that had landfill gas mitigation systems in place, suggesting that the effectiveness of these mitigation activities need to be verified by atmospheric measurement.

While we were able to make facility-level measurements to identify sources and C₂H₆/CH₄ ratios of urban CH₄ emissions, we acknowledge that a major drawback to on-road sampling is the challenge of making representative measurements. Local atmospheric CH₄ levels strongly depend on proximity to emissions source; however, we were not always able to directly access CH₄ emitting facilities, such as inside oil refineries or on landfill surfaces. Here we used measurements away from CH₄ emission sources (local background air) to overcome the limitations of our sampling approach. For this reason, quantitative flux estimates from mobile laboratory sampling in urban areas is extremely challenging. Future studies can reduce this bias by combining multiple techniques along with on-road sampling, including continuous measurement from tall towers, aircraft and total column trace gas measurements along with direct flux measurements such as chambers or eddy covariance. Another potential bias in our sample may be due to more extensive coverage in the western portions of the basin, which are densely populated, and have the most concentrated oil and gas infrastructure.

Mobile laboratory sampling has significant cost and logistic advantages over aircraft. Unlike aircraft, mobile measurements are also able to target specific CH₄ sources and observe a variety of source mixtures. Nevertheless, proximity to emissions sources can also be a disadvantage. Aircraft and remote sensing studies can use the relationship between CH₄ and CO or CO₂ in regionally representative air masses, along with inventories of those gases to estimate CH₄ emissions [e.g., Wennberg *et al.*, 2012; Wong *et al.*, 2015]. With on-road sampling, however, we found poor relationships between CH₄ and CO, and CH₄ and CO₂, even in well-mixed local background air, likely due to our proximity to on-road sources of CO and CO₂. We found no evidence of vehicle emissions on our CH₄ and C₂H₆ measurements. No CH₄ hotspots coincided with areas of high traffic emissions, including roadway tunnels.

4.3 Urban pattern of CH₄ (and C₂H₆) distinct from CO, CO₂

The differing spatial patterns of these 4 long-lived trace gases demonstrate that different measurement, monitoring, and mitigation approaches are needed for different urban greenhouse gases. Excess CH₄ was relatively concentrated in space compared to CO₂, and large CH₄ enhancement measured in the vicinity of the strongest hotspots suggest they contribute significantly to basin-wide CH₄ emissions. It may be easier for mitigation efforts to target these point emission sources to achieve equivalent reduction in radiative forcing as reducing more diffuse CO₂ emissions from a whole system. More work is needed to quantify the relative importance of emissions from these CH₄ hotspots.

In addition to monitoring hotspots, the discrepancy between inventory and atmospheric measurement also suggests that wide-ranging measurements must also be made to capture the

effects of distributed CH₄ sources. We observed basin-wide enhancement of atmospheric CH₄ levels, a so-called urban dome, but found that the distribution of CH₄ within the city is more strongly controlled by proximity to myriad emission sources. The mobile laboratory approach demonstrated that these points of emission can be linked with individual emitters and attributed to anthropogenic sources. The repeatability of hotspot locations suggests that there are significant, discrete CH₄ emissions sources that can be targeted by mitigation efforts. Future work is needed to determine the mechanisms of these leaks (e.g., pipeline seam weld leaks vs. fitting leaks), the cost of repair, and an effective strategy for reducing the most critical CH₄ sources. Finally, the fine spatial scales of 10s to 100s of meters at which CH₄ hotspots occur suggests that a mobile sampling strategy should be an integral part of a city or regional scale greenhouse gas measurement effort.

Acknowledgements

Original geo-located, time stamped trace gas measurements made by mobile laboratory are provided as Data Set S1. This research is funded by US Department of Energy's Office of Science (BER) under Grant No. DE-SC0005266. This work was supported in part by the W. M. Keck Institute for Space Studies. We thank Valerie Carranza, Joshua Miu, Mariela Ruacho, Kristal Verhulst, Josette Marrero, and Tianyang Zhu for help with field work, and Simone Meinardi for help in the laboratory.

References

- Aydin, M., K.R. Verhulst, E.S. Saltzman, M.O. Battle, S.A. Montzka, D.R. Blake, Q. Tang, and M.J. Prather (2011), Recent decreases in fossil-fuel emissions of ethane and methane derived from firn air, *Nature*, 476, 198-201.
- Bilodeau, W.L., S.W. Bilodeau, E.M. Gath, M. Osborne, and R.J. Proctor (2007), Geology of Los Angeles, California, United States of America, *Environmental & Engineering Geoscience*, XIII (2), 99-160.

Blake, D.R., V.H. Woo, S.C. Tyler, and F.S. Rowland (1984), Methane mole fractions and source strengths in urban locations, *Geophysical Research Letters*, *11*, 1211-1214.

Brandt, A.R., et al. (2014), Methane leaks from North American natural gas systems, *Science*, *343*, 733-735.

Bush, S.E., F.M. Hopkins, J.T. Randerson, C.T. Lai, J.R. Ehleringer (2015), Design and application of a mobile ground-based observatory for continuous measurements of atmospheric trace-gas and criteria pollutant species, *Atmospheric Measurement Techniques*, *8*, 3481-3492.

California Air Resources Board (CARB), (2011), California Greenhouse Gas Emissions Inventory. California Air Resources Board Staff Report (<http://www.arb.ca.gov/cc/inventory/inventory.htm>, document: ghg_inventory_by_ipcc_00-09_2011-10-26.xls)

California Air Resources Board Air Quality Planning and Science Division, (2014), Greenhouse Gas Emissions Inventory Technical Support Document, 2014 Edition (http://www.arb.ca.gov/cc/inventory/doc/methods_00-12/ghg_inventory_00-12_technical_support_document.pdf)

Cardno ENTRIX (2012), Hydraulic Fracturing Study, PXP Inglewood Oil Field, report, 206 pp., Plains Exploration & Production Company and Los Angeles County, Department of Regional Planning, Los Angeles, CA

Cicerone, R.J., and R.S. Oremland (1988), Biogeochemical aspects of atmospheric methane, *Global Biogeochem. Cycles*, *2*, 299-327.

Colman, J.J., A.L. Swanson, S. Meinardi, B.C. Sive, D.R. Blake, and F.S. Rowland (2001), Description of the Analysis of a Wide Range of Volatile Organic Compounds in Whole Air Samples Collected during PEM-Tropics A and B, *Analytical Chemistry*, *73*, 3723-31.

Djuricin S., D.E. Pataki, and X. Xu (2010), A comparison of tracer methods for quantifying CO₂ sources in an urban region, *J. Geophys. Res.*, *115*, D11303, doi:10.1029/2009JD012236.

Dlugokencky, E.J., P.M. Lang, K.A. Masarie, A.M. Croswell, and M.J. Croswell (2013a), Atmospheric Carbon Dioxide Dry Air Mole Fractions from the NOAA ESRL Carbon Cycle Cooperative Global Air Sampling Network, 1968-2012, Version: 2013-08-28, Path: ftp://aftp.cmdl.noaa.gov/data/trace_gases/co2/flask/surface/co2_kum_surface-flask_1_ccgg_event.txt

Dlugokencky, E.J., P.M. Lang, A.M. Croswell, K.A. Masarie, M.J. Croswell (2013b),

Atmospheric Methane Dry Air Mole Fractions from the NOAA ESRL Carbon Cycle Cooperative Global Air Sampling Network, 1983-2012, Version: 2013-08-28;, Path: ftp://aftp.cmdl.noaa.gov/data/trace_gases/ch4/flask/surface/ch4_kum_surface-flask_1_ccgg_event.txt

Etiopio, G., and P. Ciccioli (2009), Earth's Degassing: a missing ethane and propane source, *Science*, 323, 478.

Farrell, P., D. Culling, and I. Leifer (2013), Transcontinental Methane Measurements: Part 1. A Mobile Surface Platform for Source Investigations, *Atmos. Env.*, 74, 422-431.

Gautier, D.L., M.E. Tennyson, R.R. Charpentier, T.A. Cook, and T.R. Klett (2012), Foregone oil in the Los Angeles Basin: Assessment of remaining petroleum in giant fields of Southern California, *Search and Discovery*, Article #20164.

GeoScience Analytical, Inc. (1986), A Study of Abandoned Oil and Gas Wells and Methane and Other Hazardous Gas Accumulations, report, 462 pp., California Department of Conservation, Division of Oil and Gas.

Gini, C. (1912), Variabilità e mutabilità, in *Memorie di metodologica statistica*, edited by E. Pizetti, T. Salvemini, Libreria Eredi Virgilio Veschi, Rome, 156 pp.

Helmig D., Hueber J., Tans P. (2011) Non-Methane Hydrocarbons from the NOAA ESRL Surface Network, 2004-2011, Path: ftp://aftp.cmdl.noaa.gov/data/trace_gases/voc/c2h6/flask/event/kum_01D0_event.c2h6

Hsu, Y.-K., T. VanCuren, S. Park, C. Jakober, J. Herner, M. FitzGibbon, D.R. Blake, and D.D. Parrish (2010), Methane emissions inventory verification in southern California, *Atmos. Env.*, 44, 1-7.

Jackson, R.B., A. Down, N.G. Phillips, R.C. Ackley, C.W. Cook, D.L. Plata, and K. Zhao (2014), Natural gas pipeline leaks across Washington, DC, *Environ. Sci. Technol.*, 48, 2051-2058.

Jeffrey, A. W. A. et al. (1991), Geochemistry of Los Angeles Basin Oil and Gas Systems, in *Active Margin Basins, Memoir 52*, edited by K. T. Biddle, pp. 197-219, Amer. Assoc. Petr. Geologists, Tulsa, Okla.

Jeong, S., Y.-K. Hsu, A.E. Andrews, L. Bianco, P. Vaca, J.M. Wilczak, and M.L. Fischer (2013), A multi tower measurement network estimate of California's methane emissions, *J. Geophys. Res.*, 118, 11339-11351, doi:10.1002/jgrd.50854.

Karion, A., et al. (2013), Methane emissions estimate from airborne measurements over a western United States natural gas field, *Geophys. Res. Lett.*, *40*, 1-5, doi:10.1002/grl.50811.

Kirchstetter, T.W., B.C. Singer, R.A. Harley, G.R. Kendall, and W. Chan (1996), Impact of oxygenated gasoline use on California light-duty vehicle emissions, *Environ. Sci. Technol.*, *30*, 661-670.

Kirschke, S., et al. (2013), Three decades of global methane sources and sinks, *Nature Geoscience*, *6*, 813-823.

Kort, E.A., J. Eluszkiewicz, B.B. Stephens, J.B. Miller, C. Gerbig, T. Nehrkorn, B.C. Daube, J.O. Kaplan, S. Houweling, S.C. Wofsy (2008), Emissions of CH₄ and N₂O over the United States and Canada based on a receptor-oriented modeling framework and COBRA-NA atmospheric observations, *Geophys. Res. Lett.*, *35*, L18808, doi:10.1029/2008GL034031

Lamb, B.K., S.L. Edburg, T.W. Ferrara, T. Howard, M.R. Harrison, C.E. Kolb, A. Townsend-Small, W. Dyck, A. Possolo, J.R. Whetstone (2015), Direct Measurements Show Decreasing Methane Emissions from Natural Gas Local Distribution Systems in the United States, *Environ. Sci. Technol.*, *49*, 5161-5169.

Leifer, I., D. Culling, O. Schneising, P. Farrell, M. Buchwitz, and J.P. Burrows (2013), Transcontinental methane measurements: Part 2. Mobile surface investigation of fossil fuel industrial fugitive emissions, *Atmos. Env.*, *74*, 432-441.

Marcotullio, P.J., A. Sarzynski, J. Albrecht, N. Schulz, and J. Garcia (2013), The geography of global urban greenhouse gas emissions: an exploratory analysis, *Climatic Change*, *121*, 621-634.

Miller, S.M., et al. (2013), Anthropogenic emissions of methane in the United States, *Proc. Natl. Acad. Sci. U.S.A.*, www.pnas.org/cgi/doi/10.1073/pnas.1314392110.

Myhre, G., D. Shindell, et al., (2013), Anthropogenic and Natural Radiative Forcing, in *Climate Change 2013: The Physical Science Basis. Contribution of Working Group I to the Fifth Assessment Report of the Intergovernmental Panel on Climate Change*, edited by T.F. Stocker, D. Qin, G.-K. Plattner, M. Tignor, S.K. Allen, J. Boschung, A. Nauels, Y. Xia, V. Bex and P.M. Midgley, Cambridge University Press, Cambridge, United Kingdom and New York, NY, USA.

Newman, S., et al. (2013), Diurnal tracking of anthropogenic CO₂ emissions in the Los Angeles Basin megacity during spring 2010, *Atmos. Chem. Phys.*, *13*, 4359-4372.

Novelli, P.C. and K.A. Masarie (2013), Atmospheric Carbon Monoxide Dry Air Mole Fractions

from the NOAA ESRL Carbon Cycle Cooperative Global Air Sampling Network, 1988-2012, Version: 2013-06-18, Path: ftp://aftp.cmdl.noaa.gov/data/trace_gases/co/flask/surface/co_kum_surface-flask_1_ccgg_event.txt

Petron, G., et al., (2012), Hydrocarbon emissions characterization in the Colorado Front Range: a pilot study, *J. Geophys. Res.*, 117, D04304.

Peischl, J., et al. (2013), Quantifying sources of methane using light alkanes in the Los Angeles Basin, California, *J. Geophys. Res.*, 118, 4974-4990, doi:10.1002/jgrd.50413.

Phillips, N.G., R. Ackley, E.R. Crosson, A. Down, L.R. Huttyra, M. Brondfield, J.D. Karr, K. Zhao, and R.B. Jackson (2013), Mapping urban pipeline leaks: Methane leaks across Boston, *Environ. Pollution*, 173, 1-4.

Rudolph, J., (1995), The tropospheric distribution and budget of ethane, *J. Geophys. Res.*, 100, 11369-11381.

Shindell, D., et al., (2012), Simultaneously mitigating near-term climate change and improving human health and food security, *Science*, 335, 183-189.

Southern California Gas Company (2011), Pipeline Safety Activities Performed by Southern California Gas Company within the County of Los Angeles, report, County of Los Angeles Department of Public Works, Los Angeles, CA

Tennyson, M. (2005). Growth History of Oil Reserves in Major California Oil Fields During the Twentieth Century, U.S. Geological Survey Bulletin 2172-H., Reston, VA.

Townsend-Small, A., S.C. Tyler, D.E. Pataki, X. Xu, and L.E. Christensen (2012), Isotopic measurements of atmospheric methane in Los Angeles, California, USA: Influence of "fugitive": fossil fuel emissions, *J. Geophys. Res.*, 117, D07308, doi:10.1029/2011JD016826.

U.S. Environmental Protection Agency (US EPA) (2014), Inventory of U.S. Greenhouse Gas Emissions and Sinks: 1990-2012, Publ. EPA 430-R-14-003, Washington, D.C.

Vutukuru, S., R.J. Griffin, and D. Dabdub (2006), Simulation and analysis of secondary organic aerosol dynamics in the South Coast Air Basin of California, *J. Geophys. Res.*, 111, D10S12, doi:10.1029/2005JD006139.

Wennberg, P.O., et al., (2012), On the sources of methane in the Los Angeles atmosphere, *Environ. Sci. Technol.*, 46, 9282-9289.

Wilks, D.S. (2011), *Statistical Methods in the Atmospheric Sciences*, 3rd Edition, p.122, Academic Press, Elsevier, Oxford, U.K.

Wong, K.W., et al., (2015), Mapping CH₄:CO₂ ratios in Los Angeles with CLARS-FTS from Mount Wilson, California, *Atmos. Chem. Phys.*, 15, 241-252.

Wunch, D., P.O. Wennberg, G.C. Toon, G. Keppel-Aleks, and Y.G. Yavin (2009), Emissions of greenhouse gases from a North American megacity, *Geophys. Res. Lett.*, 36, L15810, doi:10.1029/2009GL039825.

Xiao, Y., J.A. Logan, D.J. Jacob, R.C. Hudman, R. Yantosca, and D.R. Blake (2008), Global budget of ethane and regional constraints on U.S. sources *J. Geophys. Res.*, 113, D21306, doi:10.1029/2007JD009415.

Yacovitch, T.I., et al., (2014), Demonstration of an Ethane Spectrometer for Methane Source Identification, *Environ. Sci. Technol.*, doi: 10.1021/es501475q

York, D., N. Evensen, M. Martínez, and J. Delgado (2004), Unified equations for the slope, intercept, and standard errors of the best straight line, *Am. J. Phys.*, 72(3), 367–375.

Author Manuscript

Figure 1. *Map of Los Angeles Basin methane sources and sampling area for June 2013 campaign.* Map depicts 33.6° to 34.3°N, and 117.3° to 118.7°W. (a) Location of major CH₄ sources in the basin. Individual sources include: oil refineries (purple spheres), oil wells (magenta and black markers), geologic seeps (magenta spheres), active and former landfills (brown shaded areas), wastewater treatment (green markers), cattle (blue markers), power plants (yellow spheres), and natural gas fueling stations (cyan markers). (b) Daytime measurements of CH₄ mole fraction, in ppm. (c) Daytime measurements of C₂H₆ mole fraction, in ppb, (d) Daytime measurements of the ratio of CH₄ to C₂H₆, expressed as mole ratio percent.

Figure 2. *Spatial distribution of urban excess CH₄, C₂H₆, CO₂, and CO by distance.* Percent contribution of ordered transect distance to trace gas excess measured over the campaign, excluding data from known CH₄ emission sources. Excess trace gas values for every 150 m road segments were ordered from largest to smallest, and binned into increments representing 1% of total distance driven over the campaign. Bars represent the percent of total trace gas excess represented by 1% of distance driven (left axis), and corresponding excess value (right axis). Inset plots show cumulative percent of total excess, starting with the highest 1% of trace gas excess values.

Figure 3. *Trace gas excess along a repeated coastal transect.*

a) Map of route along Pacific Coast Highway beginning at 33.61° N, 117.89° W and ending at 33.76° N, 117.11 W°. Location of UC Irvine is represented by yellow pin in upper righthand corner. (b) Excess CH₄, (c) excess CO₂, (d) excess CO, and (e) winds, measured at five different times. Orange highlighted section of map and plots shows section of road passing through a natural reserve (salt marsh), while the remainder of road passed through urbanized land.

Figure 4. *Spatial distribution of CH₄ compared to distribution of C₂H₆ at the same locations.*

Distribution of excess CH_4 values in unknown CH_4 hotspots and local background air by distance traveled. Height of bars represents percent of excess CH_4 for each 1% of distance traveled (blue bars), and corresponding percent of excess C_2H_6 for the same locations (red bars).

Figure 5. *Fossil source tracers for CH_4 and CO_2 .* a) Distribution of $\text{C}_2\text{H}_6/\text{CH}_4$ (mole ratio %) as a fraction of excess CH_4 measured during the June campaign, excluding data from known CH_4 emission sources, b) distribution of CO/CO_2 (mole ratio %) as a fraction of total excess CO_2 measured. The top 5% of CO_2 data with respect to CO/CO_2 values is not shown for scaling reasons.

Figure 6. *$\text{C}_2\text{H}_6/\text{CH}_4$ relationship for source apportionment.* Excess $\text{C}_2\text{H}_6/\text{CH}_4$ values for all known hotspots (a), unknown hotspots (b), and well mixed local background air (c). For known hotspots, data collected at biogenic CH_4 sources is indicated by red dots, and data collected at fossil CH_4 sources is indicated by blue circles. Solid lines show criteria slope values, showing the maximum biogenic slope (red) and minimum fossil slope (blue). Dashed lines are best-fit lines for known biogenic (red) and fossil (blue) hotspots. For unknown hotspots and local background air, data is plotted with blue circles. Values attributed to biogenic sources are marked with red dots, and values attributed to fossil sources are marked with green dots. Insets show same data for a, b, c; but at a reduced scale.

Figure 7. *$\text{C}_2\text{H}_6/\text{CH}_4$ relationship for simultaneous aircraft and on-road sampling.* $\text{C}_2\text{H}_6/\text{CH}_4$ relationship for data collected by aircraft and on-road sampling on June 17, 18, 19, 2013, shown with magenta, green, and blue symbols, respectively. Upper panel shows a map of on-road sampling (star icons) and aircraft sampling (airplane icons) for each day. Bottom panel shows the $\text{C}_2\text{H}_6/\text{CH}_4$ ratios observed on-road (asterisks) and their slope for each sampling day (solid lines), with one standard error of the best fit line shown as the darker shaded area. Aircraft data (colored circles around yellow crosses) and their slopes (dashed line) are also shown with one standard error of the best fit line as lighter shaded area.

Figure 8. *Simulated distributions of C_2H_6/CH_4 ratios for mixing of biogenic and different fossil CH_4 sources.* The distribution of the local background air C_2H_6/CH_4 (mole ratio %; after removing known and unknown hotspots) is represented by the black line. The model with two source mixtures with an average fossil end-member ratio from combined natural gas and geologic sources is shown by a dashed red line; for natural gas sources alone, by a dashed blue line; and for geologic sources alone, by a dashed magenta line. A three-source mixture model with separate end-member ratios for biogenic, natural gas, and geologic sources is shown by a dotted cyan line.

Author Manuscript

Table 1. Summary of biogenic CH₄ hotspots associated with individual facilities or sites

Source type	Facility /site	Date(s)	Time of day	Latitude	Longitude	Hotspot extent (km)	Average excess CH ₄ (ppm) ^a	Max. excess CH ₄ (ppb)	Max. excess C ₂ H ₆ (ppb)	C ₂ H ₆ /CH ₄ slope (%) ^b	Sample size (n)	R ² value	p value
<i>Biogenic sources</i>													
Active landfills	Puente Hills	22 June	am, pm	34.02	-118.00	10.14	1.5 ± 2.2	2725	5.9	0.02 ± 0.01	191	0.04	<0.01
	Scholl Canyon	22 June	am	34.16	-118.19	0.92	0.8 ± 0.4	3159	2.2	0.00 ± 0.01	46	0.04	0.21
Former landfills	UCI landfill	24 June	am	33.654	-117.86	0.44	0.12 ± 0.03	2866	0.5	0.00 ± 0.01	33	0.00	0.76
	Palos Verdes landfill	24 June	am	33.79	-118.35	1.39	0.5 ± 0.5	1392	1.3	-0.03 ± 0.02	28	0.11	0.09
	Cal Compact landfill	19, 23, 26 June	am, pm	33.84	-118.27	1.93	0.4 ± 0.2	1811	5.6	-0.13 ± 0.08	48	0.02	0.30
Cattle	Chino	18, 27 June	am, pm	33.99	-117.63	8.86	3.8 ± 9.4	13246	23.4	0.00 ± 0.00	977	0.00	0.84
Water treatment	Mesa Water District colored water treatment plant	14, 15, 19, 22, 23, 24, 26, 27 June, 5 July	am, pm	33.687	-117.914	5.3	0.7 ± 0.5	7768	4.3	0.02 ± 0.01	137	0.09	<0.01
	Orange County Sanitation District reclamation plant 1	14, 19, 23, 24, 26, 27 June, 5 July	am, pm	33.69	-117.94	2.0	0.3 ± 0.1	1433	9.9	0.50 ± 0.05	77	0.40	<0.01

^a Reported error is one standard deviation of the mean

^b Slope is calculated by orthogonal distance regression, reported error is the larger of error estimates for slope from orthogonal distance regression and ordinary linear regression

Table 2. Summary of natural gas CH₄ hotspots associated with individual facilities or sites

Source type	Facility /site	Date(s)	Time of day	Latitude	Longitude	Hotspot extent (km)	Average excess CH ₄ (ppm) ^a	Max. excess CH ₄ (ppb)	Max. excess C ₂ H ₆ (ppb)	C ₂ H ₆ /CH ₄ slope (%) ^b	Sample size (n)	R ² value	p value
<i>Fossil sources: fugitive natural gas leaks</i>													
Power plants	Haynes steam plant	14, 27 June	am, pm	33.76	-118.096	15.0	0.07 ± 0.02	312	4.5	3.1 ± 0.5	19	0.24	0.03
	AES Alamitos	22 June	pm	33.77	-118.10	0.8	0.27	482	9.7	3.8 ± 0.3	50	0.36	<0.01
	NRG	23 June	am	33.91	-118.425	0.4	0.29	1256	29.2	2.5 ± 0.7	5	0.61	0.12
CNG fueling stations	Clean Energy headquarters	17, 23, 24, 26 June	am, pm	33.774	-118.077	1.9	0.3 ± 0.4	1110	30.5	3.1 ± 0.1	38	0.94	<0.01
	Clean Trucks, Port of Long Beach	24 June	am	33.783	-118.222	0.9	2.1 ± 3.0	58425	479.7	0.87 ± 0.03	141	0.81	<0.01
	Clean Energy Newport Beach	14 June	am	33.632	-117.927	0.6	0.1	203	1.8	1.2 ± 0.3	12	0.35	0.04
	PH ^c landfill truck gas fueling	22 June	am	34.023	-118.028	0.6	2.2	11365	117.0	0.9 ± 0.1	32	0.49	<0.01

Natural gas pipelines under roads	Pacific Coast Hwy at Superior, NB ⁺	5 July	am, pm	33.623	-117.939	1.3	0.05 ± 0.01	315	9.5	2.8 ± 0.5	50	0.25	<0.01
	Santa Ana Ave., Costa Mesa	15 June, 5 July	am, pm	33.637	-117.911	3.0	0.06 ± 0.03	490	31.1	1.8 ± 0.1	74	0.27	<0.01
	Goldenwest St., Huntington Beach	15 June	am	33.74	-118.007	0.3	0.29	720	16.9	2.1 ± 0.1	56	0.80	<0.01
	Campus and Carlson, Irvine	16 June	am	33.664	-117.851	0.5	0.18	248	3.0	2.1 ± 0.5	5	0.78	0.04
	91 Fwy at Buchanan, Corona	16 June	am	33.895	-117.50	0.9	0.3	316	4.1	1.9 ± 0.6	8	0.96	<0.01

Source type	Facility /site	Date(s)	Time of day	Latitude	Longitude	Hotspot extent (km)	Average excess CH ₄ (ppm) ^a	Max. excess CH ₄ (ppb)	Max. excess C ₂ H ₆ (ppb)	C ₂ H ₆ /CH ₄ slope (%) ^b	Sample size (n)	R ² value	p value
<i>Fossil sources: geologic sources and fossil fuel production</i>													
Oil refineries	Conoco Phillips	24 June	am	33.778	-118.29	0.3	0.24	1781	38.9	2.8 ± 0.5	11	0.54	<0.01
	BP	23, 26 June	am, pm	33.82	-118.24	2.6	0.24 ± 0.01	347	8.8	3.5 ± 0.4	24	0.45	<0.01
	Exxon	17 June	am	33.85	-118.32	2.4	0.13	559	17.3	4.0 ± 0.2	116	0.64	<0.01
	Chevron	19, 23 June	am	33.91	-118.40	3.1	0.2 ± 0.2	1101	9.6	1.1 ± 0.1	69	0.35	<0.01

Oil fields	Newport Beach	14, 15, 17 June, 5 July	am, pm	33.626	-117.946	0.9	0.09 ± 0.03	223	1.7	-0.1 ± 0.1	35	0.00	0.79
	Huntington Beach	15 June	am	33.687	-118.005	2.8	0.09 ± 0.03	352	3.2	1.1 ± 0.2	20	0.47	<0.01
	Seal Beach	14, 17, 24 June	am, pm	33.76	-118.11	1.4	0.2 ± 0.2	623	39.0	7.2 ± 0.6	38	0.48	<0.01
	Long Beach	17, 24, 26 June	am, pm	33.81	-118.17	34	0.3 ± 0.1	855	19.4	2.7 ± 0.1	79	0.75	<0.01
	Santa Fe Springs	22 June	am	33.943	-118.065	1.5	0.08 ± 0.02	1111	9.9	0.67 ± 0.05	118	0.48	<0.01
	Inglewood	26 June	pm	34.00	-118.37	0.2	0.16	653	39.2	9 ± 5	3	0.58	0.45
Geologic seeps	Holmwood & Broad, NB ^d	5 July	am, pm	33.626	-117.924	0.4	0.14 ± 0.03	1352	2.3	0.01 ± 0.02	68	0.01	0.45
	Playa Vista	19, 23 June	am, pm	33.973	-118.421	5.3	5 ± 9	27201	65.6	0.14 ± 0.01	405	0.70	<0.01
	La Brea tarpits	19, 26 June	am, pm	34.063	-118.355	1.8	1 ± 1	5021	23757	4.04 ± 0.08	615	0.58	<0.01

Table 3. Summary of geologic CH₄ hotspots associated with individual facilities or sites

^c PH: Puente Hills

^d NB: Newport Beach

Source category	Emitters sampled	C ₂ H ₆ /CH ₄ slope (%) ^a	Percent of total campaign distance driven
<i>Biogenic sources</i>			
Active landfills	2	0.01 (0.01)	0.4
Former landfills	3	-0.05 (0.08)	0.5
Cattle	1 ^b	0.00 (0.00)	1.5

Water treatment	1 ^c	0.02 (0.01)	1.1
Biogenic average	7^c	0.05 (0.03)	3.5
<i>Fossil sources: fugitive natural gas leaks</i>			
Power plants	3	3.1 (0.9)	0.1
CNG fueling stations	4	1.5 (0.3)	0.4
NG pipeline leaks	5	2.1 (0.9)	0.3
<i>Natural gas average</i>	<i>12</i>	<i>2.2 (0.4)</i>	<i>0.8</i>
<i>Fossil sources: geologic sources and fossil fuel production</i>			
Oil refineries	4	2.9 (0.7)	0.4
Oil drilling	6	3.4 (5.0)	0.6
Geologic leaks	3	1.4 (0.1)	0.7
<i>Geologic source average</i>	<i>13</i>	<i>2.8 (1.4)</i>	<i>1.7</i>
Fossil average	25	2.5 (1.1)	2.5

Table 4. Sectoral CH₄ hotspot characteristics

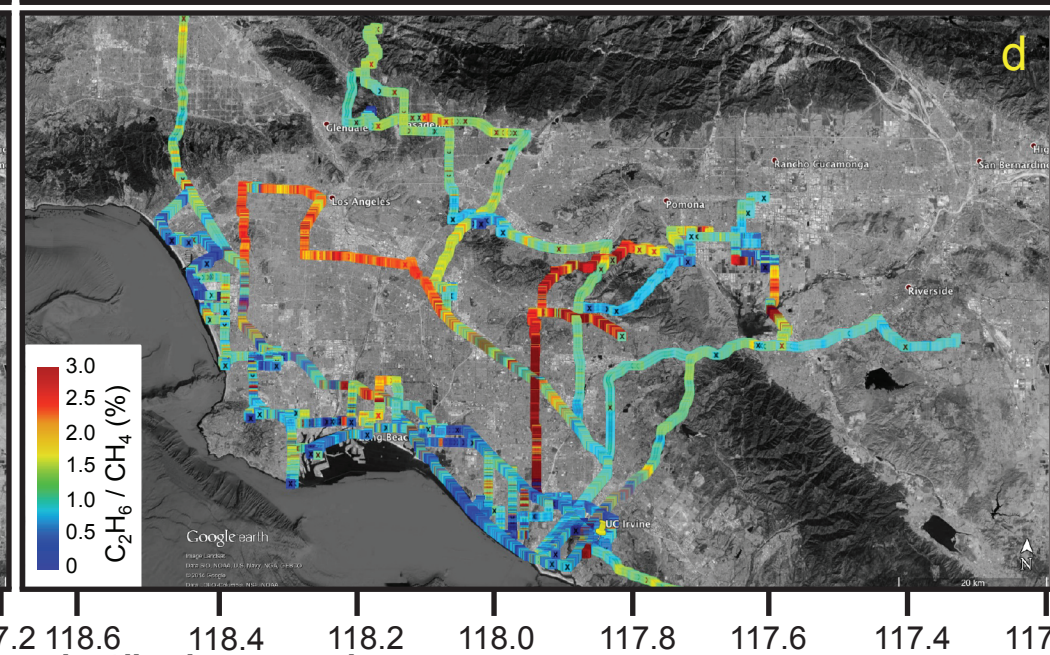
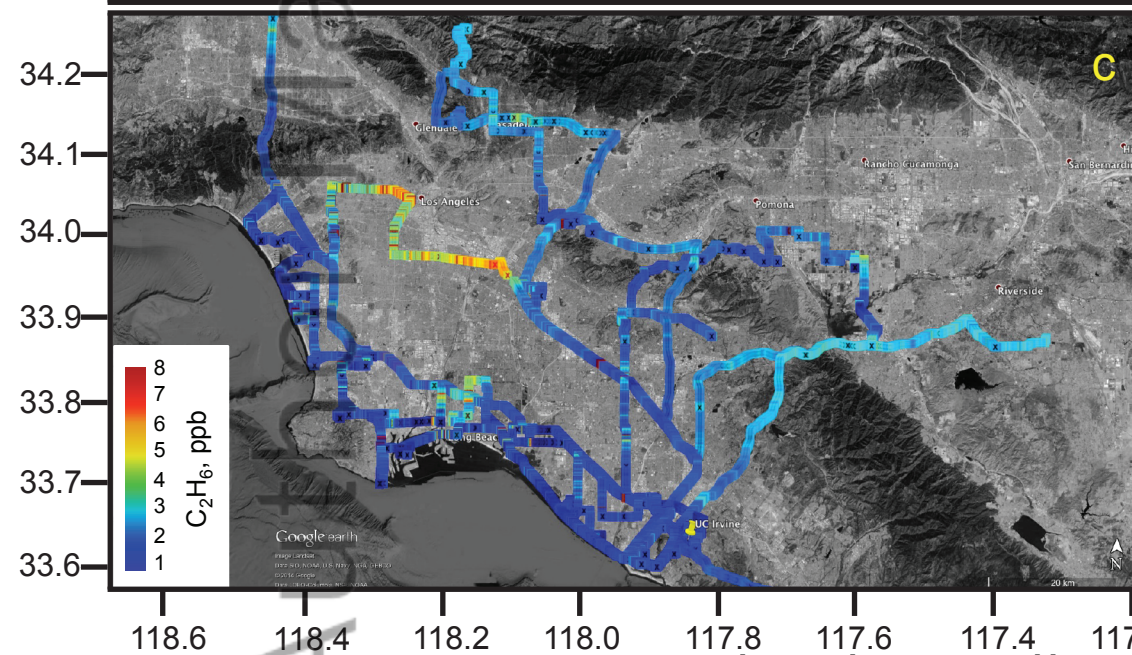
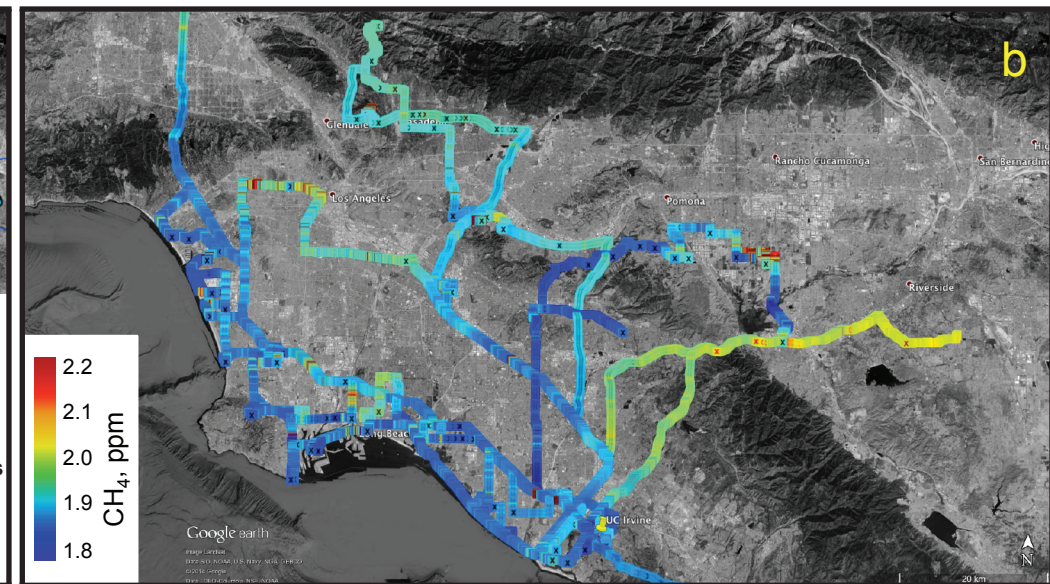
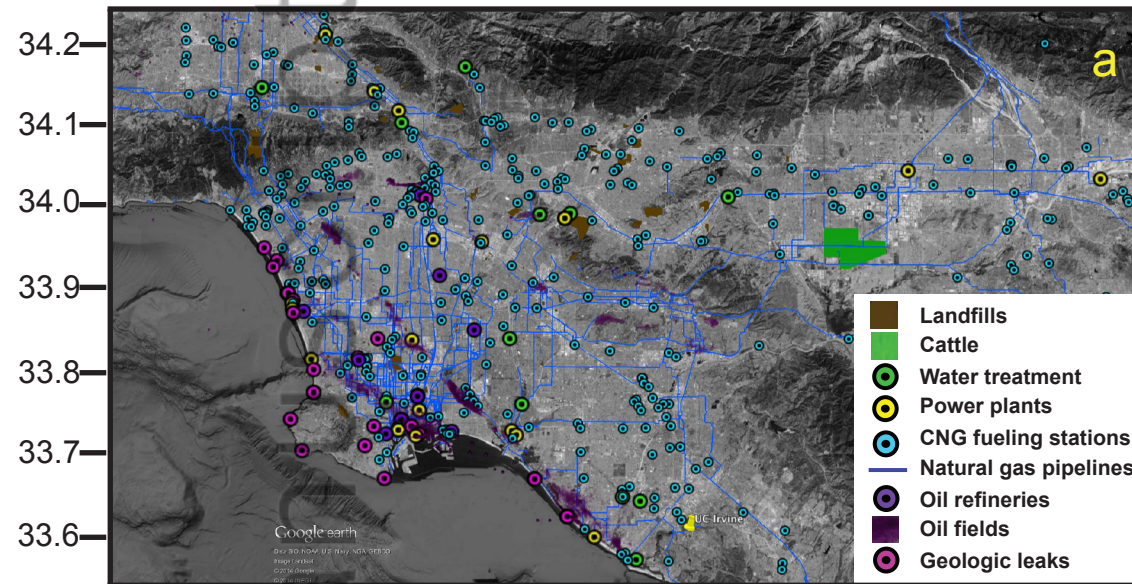
^a Slope is calculated as the average of C₂H₆/CH₄ for each emitter sampled, error on slope is propagated from error reported in Table 1

^b Single region of cattle influence, includes multiple individual dairies

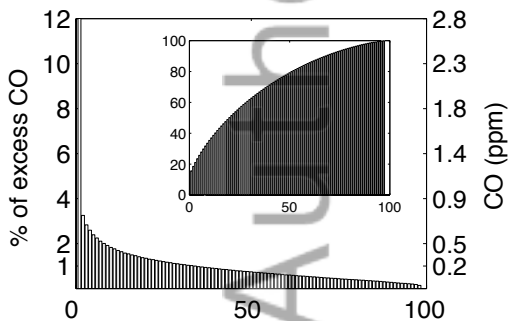
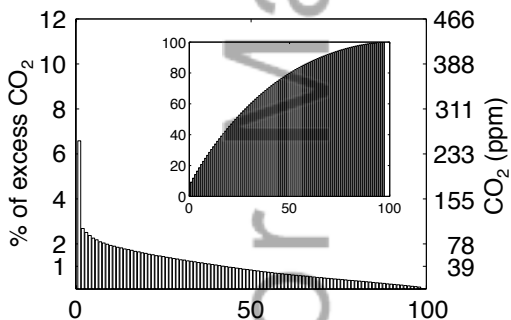
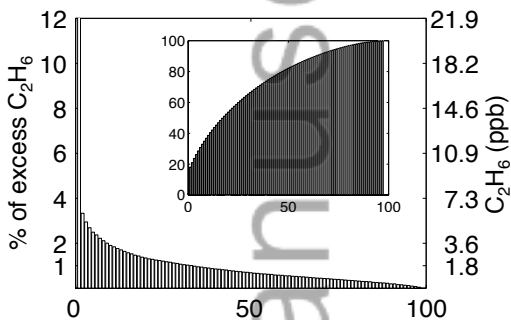
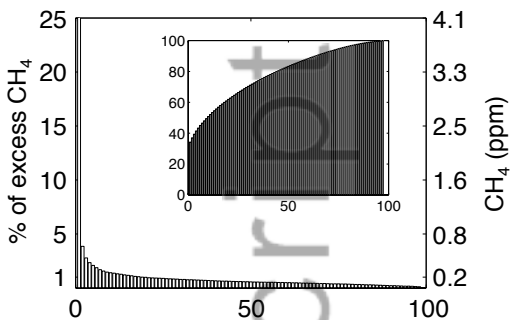
^c Excludes 1 water treatment plant with suspected fossil emissions (Orange County Sanitation District plant 1)

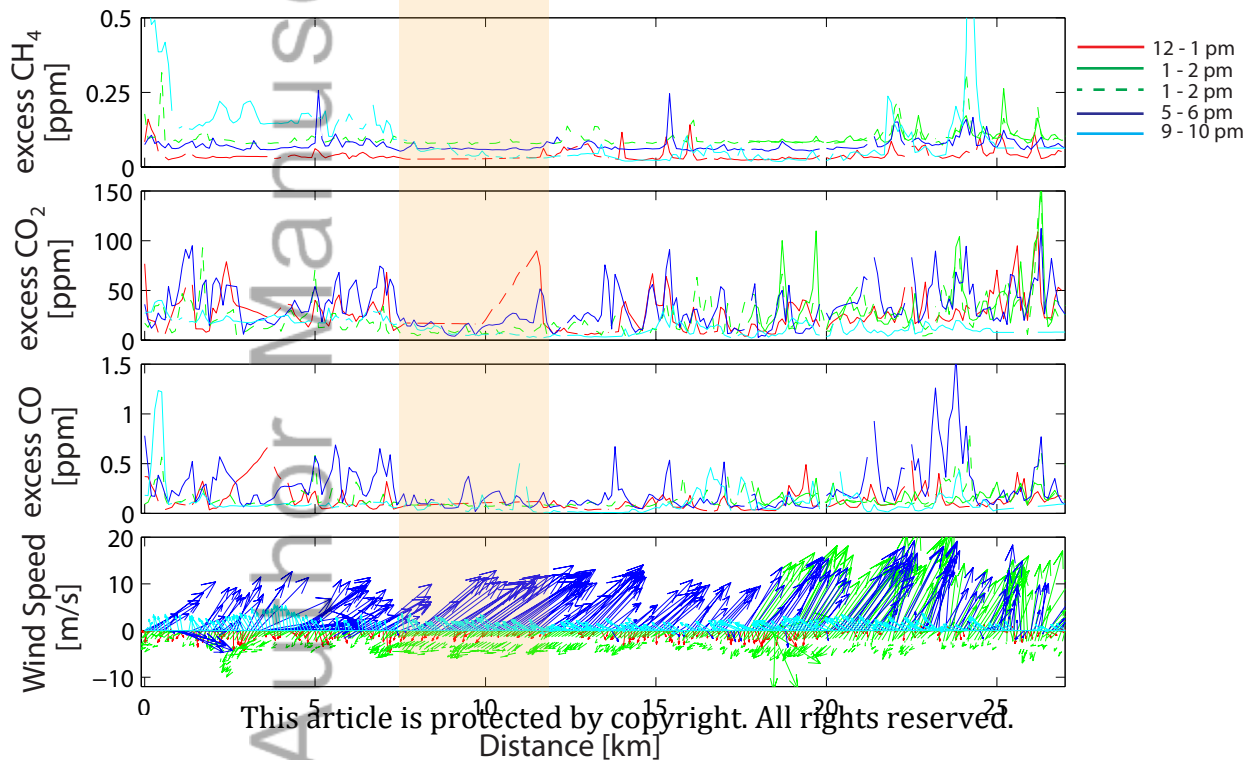
Author Manuscript

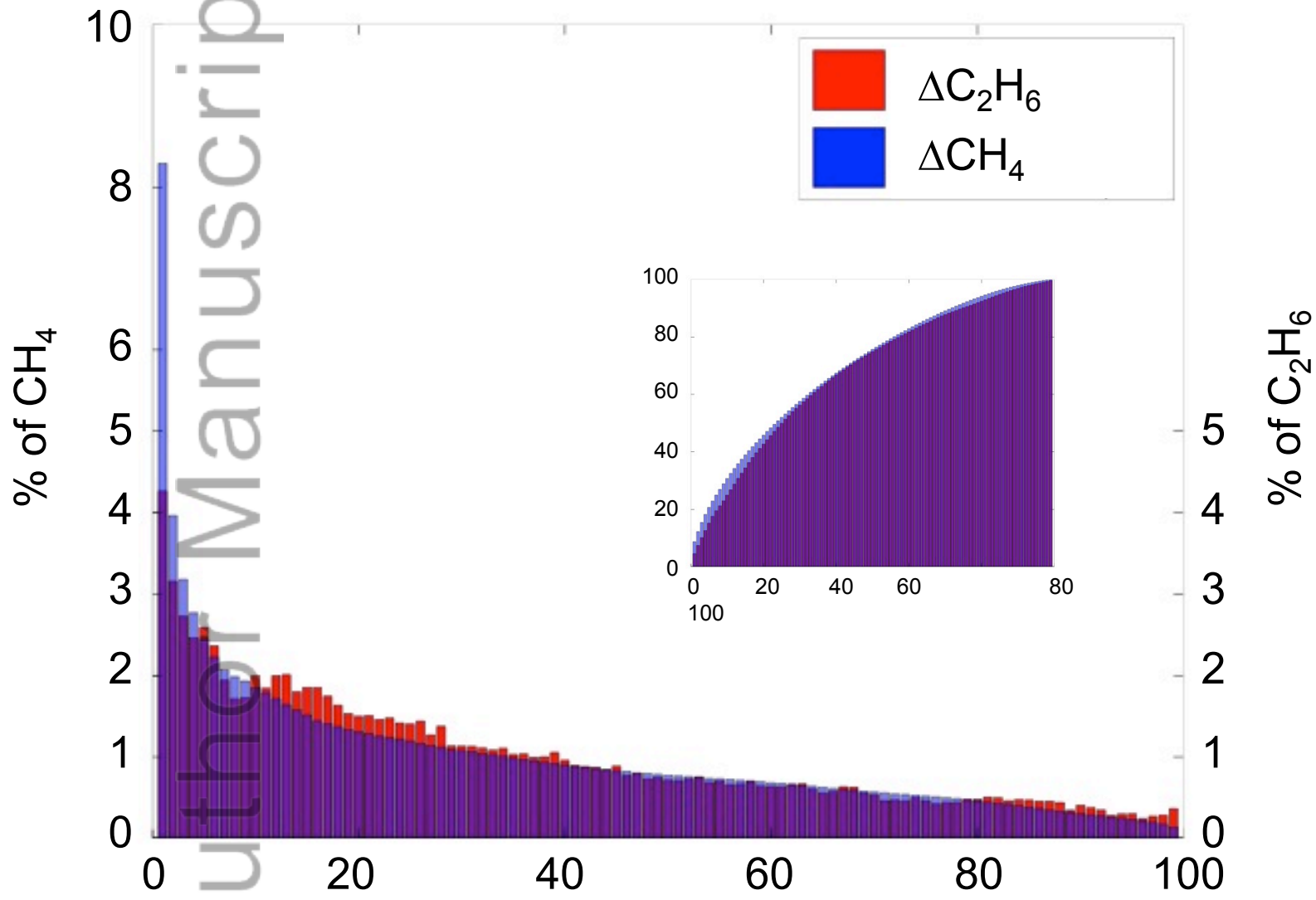
Author Manuscript

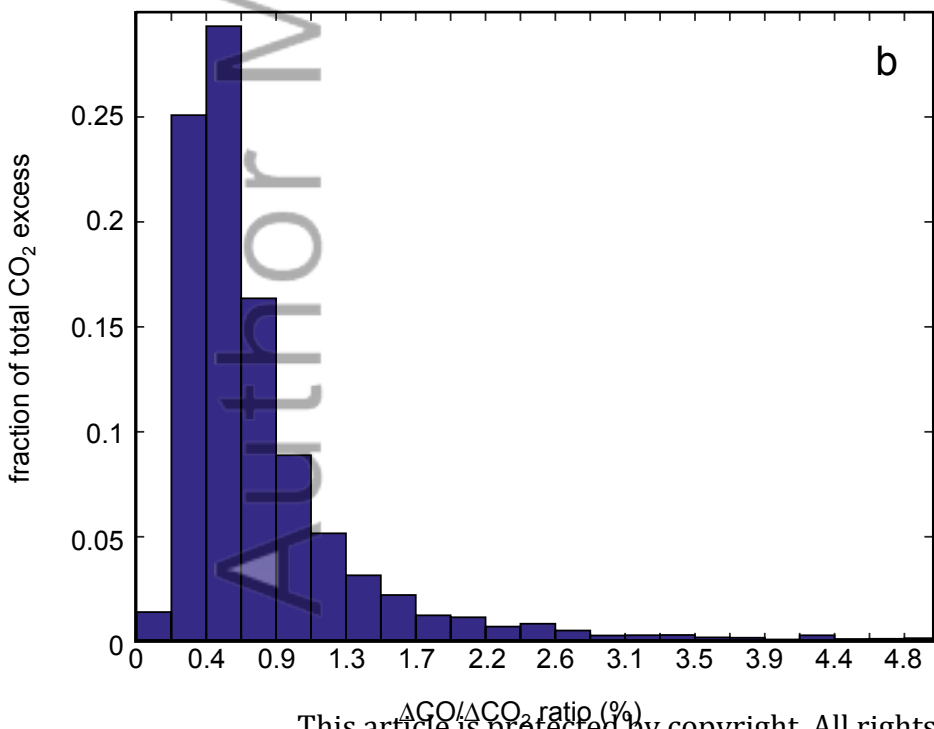
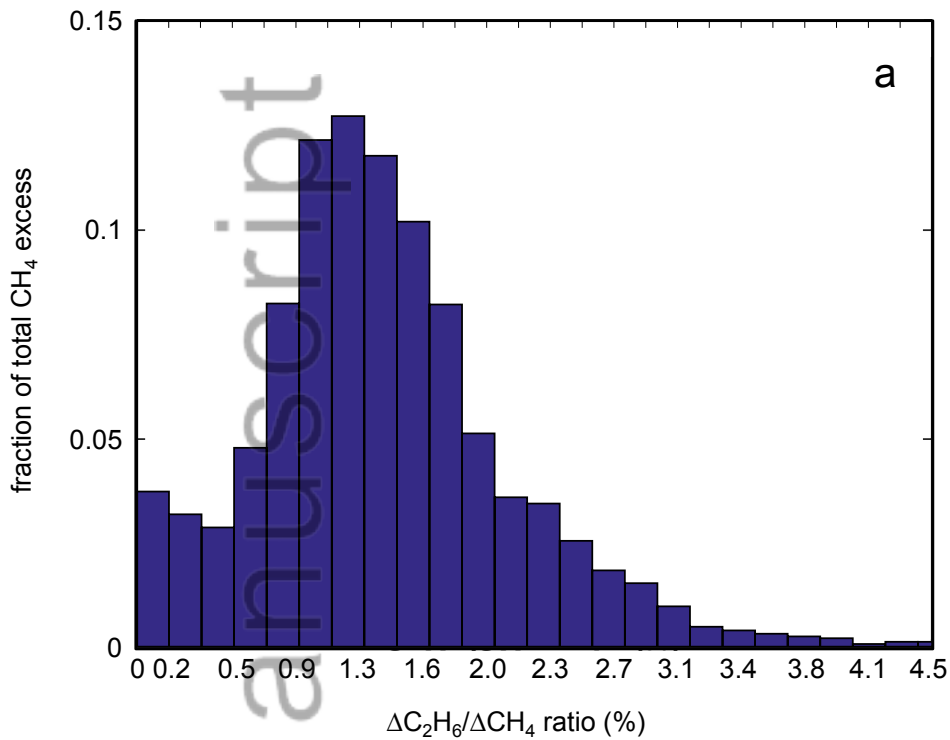


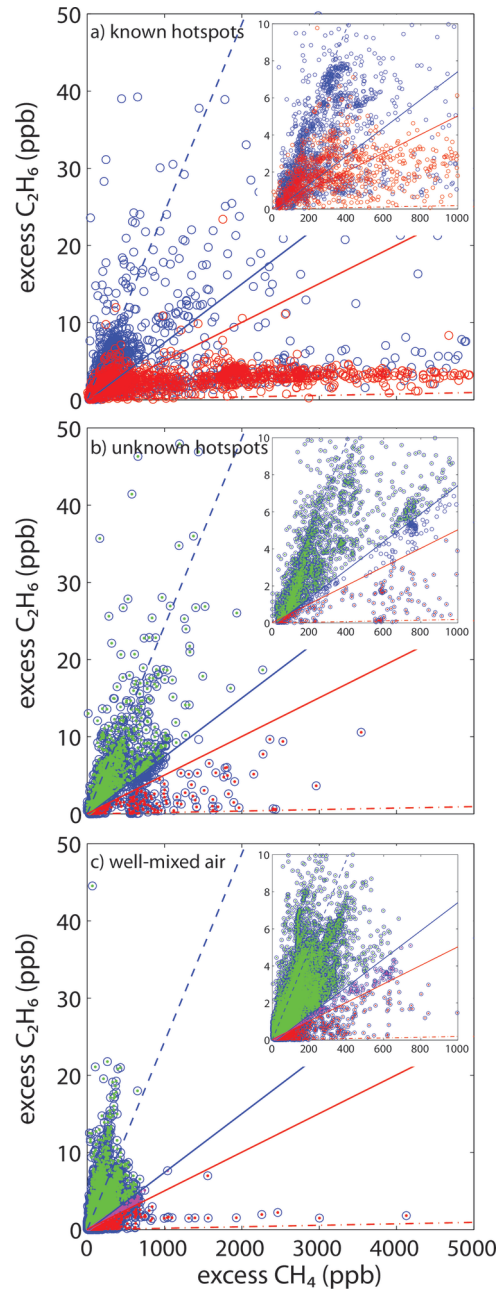
118.6 118.4 118.2 118.0 117.8 117.6 117.4 117.2 118.6 118.4 118.2 118.0 117.8 117.6 117.4 117.2











2015jd024429-f05-z-

